Journal of Materials Chemistry

Cite this: *J. Mater. Chem.*, 2011, **21**, 6251

www.rsc.org/materials

PAPER

Graphene-like MoS_2/amorphous carbon composites with high capacity and excellent stability as anode materials for lithium ion batteries

Kun Chang,[a] Weixiang Chen,*[a] Lin Ma,[b] Hui Li,[a] He Li,[c] Feihe Huang,[a] Zhude Xu,[a] Qingbo Zhang[d] and Jim-Yang Lee[d]

Received 12th January 2011, Accepted 18th February 2011
DOI: 10.1039/c1jm10174a

A facile process to synthesize graphene-like MoS_2/amorphous carbon (a-C) composites was developed. MoS_2/C composites were firstly prepared by hydrothermal method employing sodium molybdate, sulfocarbamide and glucose as starting materials. The graphene-like MoS_2/a-C composites were obtained after annealing at 800 °C in H_2/N_2. The samples were characterized by XRD, SEM, EDS and HRTEM. It was confirmed that in the composites MoS_2 has a structure of single-layer, which is named graphene-like nanostructure. The graphene-like MoS_2 nanosheets were uniformly dispersed in amorphous carbon. The interlaminar distance of the adjacent graphene-like MoS_2 nanosheets in the composites measured was ~1.0 nm. The mechanism of the formation of the graphene-like MoS_2/a-C composites was investigated. The graphene-like MoS_2/a-C composites exhibited high capacity and excellent cyclic stability used as anode materials for Li-ion batteries. The composite prepared by adding 1.0 g of glucose in hydrothermal solution exhibited the highest reversible capacity (962 mAh g^{-1}) and excellent cyclic stability. After 100 cycles, it still retained 912 mAh g^{-1}. The significant improvements in the electrochemical properties of the graphene-like MoS_2/a-C composites could be attributed to the graphene-like structure of the MoS_2 nanosheets and the synergistic effects of graphene-like MoS_2 and amorphous carbon.

Introduction

The lithium ion battery (LIB) is one of the most important rechargeable energy storage technologies, and can be used for a variety of mobile equipment, including cell phones, laptop computers and power tools. It is also a promising candidate for power sources of electric vehicles.[1–4] Graphitic materials are extensively spread as commercial anode materials for LIB due to their flat potential profile *versus* lithium and structural stability during cycling. However, graphite suffers from a relatively small capacity (372 mAh g^{-1}). In recent years, graphene, a flat one-atom-thick monolayer which is exfoliated from graphite and owns outstanding electronic behavior, large surface area and amazing mechanical properties, has attracted a great deal of research interest for many applications. In particular, the electrochemical properties of graphene nanosheets and their composites as anode materials for LIB have been intensively investigated.[5–8] High capacities from about 600–1000 mAh g^{-1} have been observed for graphene nanosheets and their composites.

In addition, the typical layered transition metal sulfides (MoS_2 and WS_2, *etc*) have an analogous structure to graphite, which are composed of three atom layers: a Mo or W layer sandwiched between two S layers, and the triple layers are stacked and held together by weak van der Waals interactions.[9,10] Precisely because of this layered structure, atoms or molecules can be embedded by intercalation methods.[11,12] The preparation of layered MoS_2 and WS_2 nanomaterials, and the investigation of their electrochemical properties have been documented.[13–16] Feng *et al.*[17] synthesized MoS_2 nanoflakes by hydrothermal methods and found that the MoS_2 nanoflakes electrodes exhibited a high insertion capacity of about 1000 mAh g^{-1}. In our previous work,[18] MoS_2 nanoflowers were synthesized by ionic liquid-assisted hydrothermal reaction. It was demonstrated that the MoS_2 nanoflowers delivered a reversible capacity of 900 mAh g^{-1}. However, the cyclic stability of the MoS_2 nanoflowers wasn't satisfactory and needed to be improved.

With the discovery and characterization of graphene, graphene analogues of layered inorganic materials such as MoS_2 and WS_2 have attracted great interest.[19] Due to their analogous structure to graphite, MoS_2 and WS_2 can also be exfoliated to single or a few layers by chemical or physical methods. Rao

[a]*Department of Chemistry, Zhejiang University, Hangzhou, PR China 310027. E-mail: weixiangchen@zju.edu.cn; Fax: (+86) 571-87951895*
[b]*Chemistry Science and Technology School, Zhanjiang Normal University, Zhanjiang, PR China 524048*
[c]*College of Biology and Environmental Engineering, Zhejiang Shuren University, Hangzhou, PR China 310015*
[d]*Department of Chemical and Biomolecular Engineering, National University of Singapore, 10 Kent Ridge Crescent, 119260, Singapore*

et al.[19] named the structure of MoS_2 and WS_2 with a single layer or a few layers graphene-like nanostructure. The exfoliation of layered MoS_2 and WS_2 has been researched for many years, but there have been only a few reports where the graphene-like MoS_2 and WS_2 were used as anode materials for LIB. Cheon *et al.*[20] synthesized graphene-like WS_2 nanosheets using $W_{18}O_{49}$ as a precursor, and found that the electrochemical lithiation capacity had been significantly improved compared to bulk WS_2. They suggested that 2D nanosheets could enhance their host capability due to the enlarged surface area and improved diffusion process upon the intercalation of guest molecules. However, the capacity of 2D-WS_2 nanosheets reported by Cheon *et al.*[20] was fading to 63% after 30 cycles, thus the cycling stability still needed to be improved. Recently, Lemmon *et al.*[21] prepared MoS_2/polyethylene oxide (MoS_2/PEO) nanocomposites by exfoliated MoS_2 and PEO. Their lithiation capacity and cycling behavior were greatly improved. Guo *et al.*[22] prepared restacked MoS_2 with enlarged *c*-parameter by exfoliation and restacking process. It was found that the restacked MoS_2 exhibited high capacity (~800 mAh g^{-1}) and superior stability. However, the exfoliation process of MoS_2 was complicated and consumed a large amount of organic reagents and took a longer time. Because of the van der Waals interactions, the exfoliated MoS_2 layers have a proneness to aggregate or restack during repetitive cycling and even in the drying process of electrodes. This would result in the loss of the unusual properties of the graphene-like MoS_2 nanosheets and negative effects on their properties. If the graphene-like MoS_2 nanosheets are uniformly dispersed in other medium such as carbon materials, their aggregation can be effectively inhibited, which leads to enhanced electrochemical properties. Therefore, a facile and efficient method is needed to synthesize graphene-like MoS_2/C composites.

In this work, we present a facile process to synthesize graphene-like MoS_2/a-C composites. MoS_2/C composites were prepared by hydrothermal route using sodium molybdate, sulfocarbamide and glucose as starting materials, and then annealing at 800 °C for 2 h in a stream of 10% hydrogen in nitrogen. Graphene-like MoS_2/a-C composites could be obtained by this process. The products were characterized by XRD, SEM, EDX and HRTEM. The results indicate that the graphene-like MoS_2 with single-layer are uniformly dispersed in amorphous carbon. The electrochemical tests demonstrate that the graphene-like MoS_2/a-C composites deliver a very high specific capacity and excellent cycle stability.

Experimental section

In a typical synthesis, 0.30 g of $Na_2MoO_4 \cdot 2H_2O$ and 0.40 g NH_2CSNH_2 were dissolved in 60 mL deionized water, and then 0.50 g, 1.00 g or 2.00 g of glucose was added into the solution. After stirring for a few minutes, the obtained clear solution was transferred into a 100 ml Teflon-lined stainless steel autoclave and sealed tightly, heated at 240 °C for 24 h. After cooling naturally, the black precipitates were collected by centrifugation, washed with deionized water and ethanol, and dried in a vacuum oven at 80 °C for 24 h. The MoS_2/C composites were annealed in a conventional tube furnace at 800 °C for 2 h in a stream of 10% hydrogen in nitrogen flowing at 200 sccm (standard cubic centimetre per minute). The annealed MoS_2/a-C composites were notated as MoS_2/a-C-0.5, MoS_2/a-C-1.0 and MoS_2/a-C-2.0. In order to investigate the effects of adding glucose into the hydrothermal solution on crystal structures and morphologies of the samples, the MoS_2 was also prepared by the hydrothermal route without adding glucose and annealed under the same conditions.

X-ray diffraction (XRD) analysis was performed using the Thermo X'TRA X-ray diffractometer with Cu Kα-source. The 2θ angular regions between 5° and 80° were investigated at a scan rate of 4° min^{-1} with a step of 0.02°. HRTEM images were obtained with JEOL JEM-2010 TEM operating at 200 kV accelerating voltage. SEM images were obtained with a SIRION-100 field emission SEM (FESEM) operating at 25 kV. The element content of the samples was analyzed by GENENIS-4000 energy dispersive X-Ray spectroscopy (EDS).

The electrochemical tests were measured *via* two-electrode cells assembled in an argon-filled glove box. Lithium sheet served as counter electrode and reference electrode, and a polypropylene film (Celgard-2300) was used as separator. The electrolyte was 1.0 M $LiPF_6$ solution in a mixture of EC/DMC (1 : 1 in volume). The working electrodes were prepared by a slurry coating procedure. The slurry consisted of 80 wt.% active material, 10 wt.% acetylene black and 10 wt.% polyvinylidene fluoride (PVDF) dissolved in *N*-methyl-2-pyrrolidinone, and was spread on a copper foil which acted as current collector. The coated electrodes were dried at 110 °C for 12 h in vacuum and then pressed. Galvanostatic charge/discharge cycles were carried out on a CBT-138-320 battery program-control test system in a voltage range of 0.01–3.00 V *vs.* Li/Li^+ at a current density of 100 mA g^{-1}.

Results and discussion

Characterization of structure and morphology

Fig. 1 shows the XRD patterns of the as-prepared MoS_2 and annealed MoS_2 synthesized by the hydrothermal method without adding glucose. Both as-prepared and annealed MoS_2 samples are single phase, as determined by the XRD patterns in Fig. 1. All reflections of both MoS_2 are in good agreement with a hexagonal structure (JCPDS 37-1492). As shown in Fig. 1, the annealed

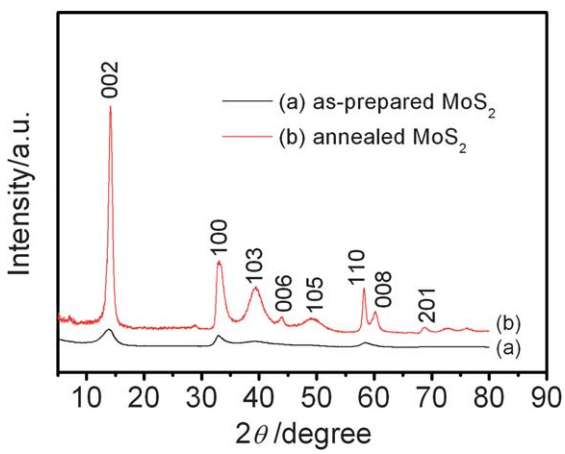

Fig. 1 XRD patterns of (a) as-prepared MoS_2 and (b) annealed MoS_2 synthesized by hydrothermal method without adding glucose.

MoS_2 shows very sharp peaks with very high intensity in comparison with the as-prepared MoS_2, and especially the strong (002) peak at $2\theta = 14.2°$ signifies a well-stacked layered structure,[23] which demonstrates that the crystallinity of MoS_2 is greatly improved after annealing.

Because the colloidal carbonaceous materials produced by the hydrothermal carbonization of glucose contained a large amount of oxygen-containing functional groups,[24] for their application as anode materials of LIB the MoS_2/C composites must be annealed at high temperature in order for the colloidal carbon to be fully carbonized. Fig. 2 shows the XRD patterns of the annealed MoS_2/a-C by hydrothermal method with addition of glucose. As shown in Fig. 2, the (002) plane peak of MoS_2 cannot be found in the annealed MoS_2/a-C composites. Only three XRD peaks at $2\theta = 33.0°$, 58.9° and 69.8° are found, which are attributed to the (100), (110) and (201) peaks of MoS_2, and the (103) peak of MoS_2 at $2\theta = 40.0°$ can be detected for MoS_2/a-C-0.5. A very weak diffraction peak at $2\theta = 25.1°$ was found, which should be attributed to the (002) plane of carbon. Because the annealing temperature of 800 °C is much lower than the graphitization temperature of 3000 °C, the carbon in the composites should be amorphous. The absence of (002) reflections of MoS_2 indicates that stacking of the single layers doesn't take place.[25] This fact indicates that the MoS_2 in the composites should have the structure of single layer or few layers, which was named graphene-like structure by Rao *et al.*[19] Thus, the annealed MoS_2/C composites are entitled graphene-like MoS_2/a-C composites in this work. This kind of graphene-like MoS_2 nanosheets could be directly observed in HRTEM images. In addition, as shown in Fig. 2, there are two new weak diffraction peaks for the graphene-like MoS_2/a-C composites near $2\theta = 10°$ and 16°, which are marked with * and #, respectively. The two peaks are indexed to neither MoS_2 nor carbon. The *d*-spacing corresponding to the two peaks of the different samples were calculated according to the diffraction angles using the Bragg equation and are summarized in Table 1. It is well known that the *d* (002)-spacing of MoS_2 and carbon are 0.62 nm and 0.33 nm, respectively. According to Fig. 1, the *d* (002)-spacing of MoS_2 is also calculated to be 0.62 nm. As shown in Table 1, the *d*-spacing of peak # is 0.49∼0.58 nm, which is between *d* (002) of MoS_2 and carbon. It is very possible that the peak # is attributed to the spacing between the MoS_2 layer and the carbon layer. The *d*-spacing of peak * is 0.97∼1.18 nm, which is just twice that of peak #, it may be the distance of adjacent MoS_2 nanosheets in amorphous carbon. This conjecture would be proven by HRTEM characterization.

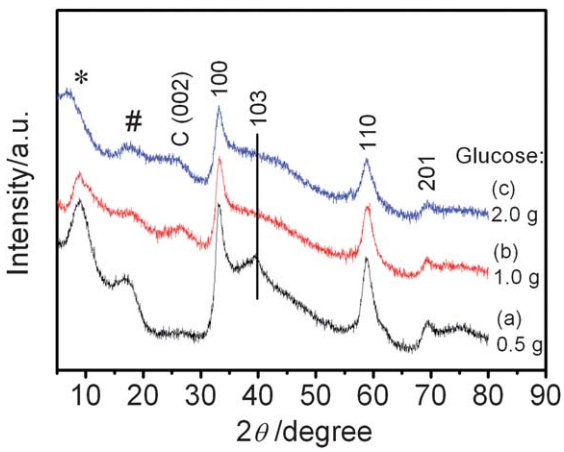

Fig. 2 XRD patterns of graphene-like MoS_2/a-C composites prepared by hydrothermal method with adding (a) 0.5 g, (b) 1.0 g and (c) 2.0 g glucose.

Table 1 *d*-spacing of the peaks (* and #) for the graphene-like MoS2/a-C composites prepared by hydrothermal route with adding various amount of glucose

Composites	2θ (°)*	*d* (nm)	2θ (°)#	*d* (nm)
MoS_2/a-C-0.5	9.1	0.97	17.2	0.49
MoS_2/a-C-1.0	8.6	1.03	16.1	0.52
MoS_2/a-C-2.0	7.5	1.18	15.7	0.58

To determine the composition of the samples, the graphene-like MoS_2/a-C composites were characterised by EDS. The element compositions of the graphene-like MoS_2/a-C composites with different carbon contents are shown in Table 2. From Table 2, it can be seen that the samples contain C, Mo, S and a small number of O. It was calculated that the atomic ratio of S and Mo is in the range of 1.94 to 2.05, which approaches the theoretical value of MoS_2. This indicates the products to be stoichiometric MoS_2. C is provided by the hydrothermal carbonization of glucose and the O is from the part that didn't reduce completely during annealing. In addition, the weight content of the MoS_2 was calculated according to Table 2 and also listed in Table 2. Table 2 shows that the weight content of the MoS_2 decreases with the increasing amount of glucose added to the hydrothermal solution.

The morphologies of the annealed MoS_2 and graphene-like MoS_2/a-C composites prepared by hydrothermal route with adding glucose are compared in Fig. 3. The SEM images give a general view of the morphology of the products over a large area. As shown in Fig. 3a, the annealed MoS_2 by hydrothermal without adding glucose consists of large micrometer-sized scaled sheets, which are stacked together. As shown in Fig. 3b, c and d, when adding glucose to the hydrothermal solution, the morphology of the graphene-like MoS_2/a-C composites interestingly changes to 3D sphere-like architecture, in which the graphene-like MoS_2 nanosheets are uniformly dispersed in the amorphous carbon. It has been reported that the carbonaceous materials produced by hydrothermal carbonization of glucose are sphere-like architectures.[26] Therefore, the glucose plays a role of spheroidizing the graphene-like MoS_2/a-C composites in the hydrothermal process.

Table 2 Composition of the graphene-like MoS2/a-C composites prepared by the hydrothermal route with addition of various amounts of glucose

	Element (wt.%)				
Composites	C	O	Mo	S	MoS_2 (wt.%)
MoS_2/a-C-0.5	22.20	13.15	38.77	25.88	64.65
MoS_2/a-C-1.0	30.15	11.49	34.59	23.76	58.35
MoS_2/a-C-2.0	38.85	10.56	31.19	19.41	50.60

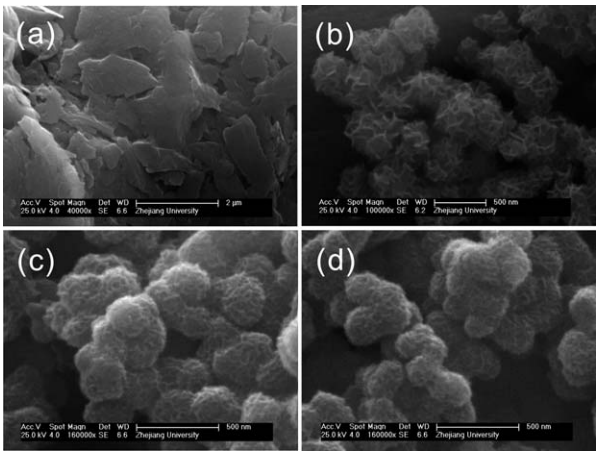

Fig. 3 SEM images of (a) annealed MoS_2 and graphene-like MoS_2/a-C composites prepared by hydrothermal method with adding (b) 0.5 g, (c) 1.0 g and (d) 2.0 g of glucose.

To further observe the microstructure, the graphene-like MoS_2/a-C composites were characterized by HRTEM. Fig. 4 shows the HRTEM images of the annealed MoS_2 and graphene-like MoS_2/a-C composites. Fig. 1(a) shows that the annealed MoS_2 displays a perfect layered crystal with an interlayer distance of the (002) plane of 0.62 nm, which is consistent with that of the literature for the hexagonal lattice of the MoS_2 phase. While after adding glucose to the hydrothermal solution, the HRTEM images of MoS_2/a-C composites in Fig. 4 (b, c and d) clearly show that the graphene-like MoS_2 nanoclusters comprised of single-layer MoS_2 dispersed in amorphous carbon, and graphene-like MoS_2 still delivers the hexagonal structure formed by Mo and S atoms with an Mo–S distance of 0.23 nm (Fig. 4c). It has been reported that the MoS_2 structure with single-layer or a few layers cannot exhibit the (002) reflection prominently,[19] so that is the reason for the absence of the (002) diffraction peak of MoS_2 for the graphene-like MoS_2/a-C in Fig. 2. The interlayer distances between MoS_2 nanosheets were measured to be 0.97, 1.03 and 1.18 nm for the graphene-like MoS_2/a-C-0.5, MoS_2/a-C-1.0 and MoS_2/a-C-2.0, respectively, which are in accordance with the results of the XRD analysis (see Fig. 2 and Table 1). Thus, it can be concluded that the diffraction peak * near $2\theta = 10^\circ$ should be attributed to the interlayer distance of the adjacent graphene-like MoS_2 nanosheets in the composites. In addition, as shown in Table 2, the plane spacing d(#) is about half the plane spacing of d(*), so we can conclude that this interlayer distance should be the one between the MoS_2 layer and the amorphous carbon. Taking the graphene-like MoS_2/a-C-1.0 composite for example, the composite microstructure is schematized in Fig. 4e. Fig. 4e shows that the MoS_2 displays a sandwich structure of S–Mo–S covalent bonds in the layer. The interlayer distance of layered MoS_2 by hydrothermal method without glucose is 0.62 nm. When adding 1.0 g of glucose to the hydrothermal route, the graphene-like MoS_2/a-C composite was obtained after annealing. As schematized in Fig. 4e, amorphous carbon exists between MoS_2 single-layers and increases the distance of the original MoS_2 layers. The interlayer distance between MoS_2 nanosheets is measured to be 1.03 nm and the interlayer distance between the MoS_2 layer and the amorphous carbon is 0.52 nm.

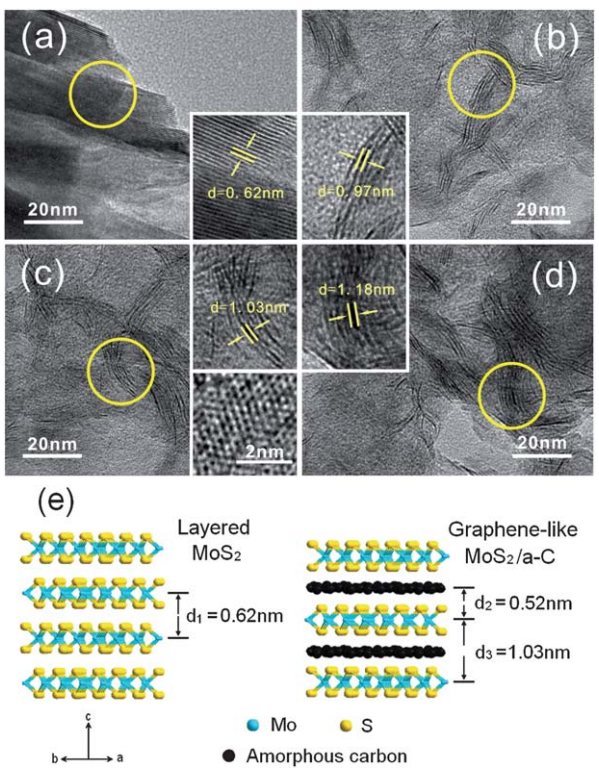

Fig. 4 HRTEM images of (a) annealed MoS_2, graphene-like (b) MoS_2/a-C-0.5, (c) MoS_2/a-C-1.0, (d) MoS_2/a-C-2.0 composites, and (e) schematic illustration of microstructures of layered MoS_2 and graphene-like MoS_2/a-C-1.0 composite.

Growth mechanism

To reveal the growth mechanism of the graphene-like MoS_2/a-C composites, the as-prepared MoS_2/C composites by the hydrothermal route with addition of 1.0 g of glucose were also characterized by SEM and XRD. Fig. 5 shows the SEM image and XRD pattern of the as-prepared MoS_2/C composite. Comparing with the XRD and SEM of the annealed MoS_2/a-C composite in Fig. 2b and 3c, it is found that the morphology of the composite before and after annealing is basically the same but the crystalline structure. As shown in Fig. 5b, the as-prepared MoS_2/C composite displays only two very weak diffraction peaks, which are attributed to the (100) and (110) planes of MoS_2.

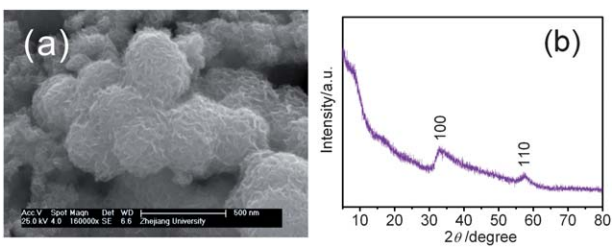

Fig. 5 (a) SEM image and (b) XRD pattern of graphene-like MoS_2/a-C composites (1.0 g glucose) by hydrothermal route without annealing.

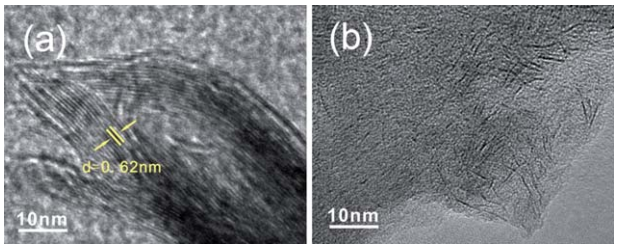

Fig. 6 HRTEM images of (a) as-prepared MoS_2 and (b) as-prepared MoS_2/C composites by hydrothermal route with addition of 1.0 g of glucose.

Fig. 6 shows the HRTEM images of the as-prepared MoS_2 and as-prepared MoS_2/C composites. As shown in Fig. 6a, a clear layered structure with $d(002) = 0.62$ nm can be found for the as-prepared MoS_2 by hydrothermal method without adding glucose. On the contrary, a layered structure of MoS_2 is hardly found for the as-prepared MoS_2/C prepared by the hydrothermal method with addition of glucose as shown in Fig. 6b. It can be seen that the MoS_2 nanowhiskers are highly dispersed in the colloidal carbonaceous material produced *in stiu* by the hydrothermal carbonization of glucose. In the hydrothermal process, the growth of MoS_2 crystals, especially in the (002) plane, is greatly inhibited due to the existing colloidal carbonaceous, so that leads to very weak diffraction peaks of (100) and (110), and the absence of (002) diffraction peak for the as-prepared MoS_2/C composite (see Fig. 5b). We can conclude that the growth mechanism of the graphene-like MoS_2/a-C composites is: whisker-like MoS_2 is firstly produced by the hydrothermal reaction between Na_2MoO_4 and NH_2CSNH_2, and highly dispersed in the colloidal carbonaceous material *in situ* produced by the hydrothermal carbonization of glucose. The colloidal carbonaceous material in the composites is further carbonized after calcination at 800 °C to change to amorphous carbon. The amorphous carbon inhibits the growth of MoS_2 crystals especially in the *c*-axis during the annealing process, which finally leads to the formation of the graphene-like MoS_2/a-C composites.

Electrochemical performance

In order to understand well the electrochemical performance of the graphene-like MoS_2/a-C composites, especially to investigate the contribution of MoS_2 and amorphous carbon to the capacity, MoS_2 and amorphous carbon were obtained by hydrothermal route and annealing at 800 °C and their electrochemical performance was also measured. Fig. 7 shows the first three charge/discharge curves of the annealed MoS_2, graphene-like MoS_2/a-C composites and amorphous carbon. As shown in Fig. 7a, two potential plateaus at ~1.1 and ~0.6 V are observed for the annealed MoS_2 electrode in the first discharge (lithiation process). The plateau at about 1.1 V is indicative of the formation of Li_xMoS_2 and the plateau variation is attributed to the lithium intercalation on different defect sites of MoS_2;[27] while the plateau at about 0.6 V can be attributed to a conversion reaction process, which first entails the *in situ* decomposition of MoS_2 into Mo particles embedded into a Li_2S matrix and then the formation of a gel-like polymeric layer resulting from electrochemically

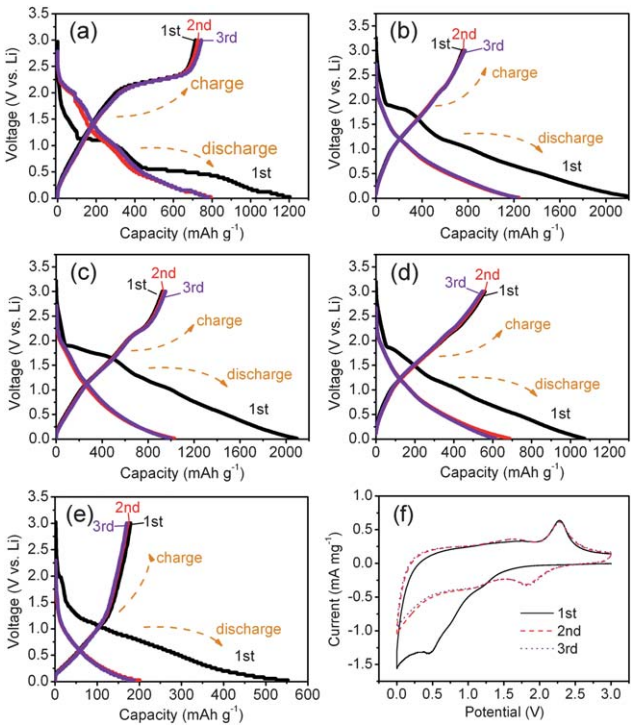

Fig. 7 First three charge/discharge curves of (a) annealed MoS_2, graphene-like (b) MoS_2/a-C-0.5, (c) MoS_2/a-C-1.0, (d) MoS_2/a-C-2.0 and (e) amorphous carbon, and (f) cyclic voltammograms of MoS_2/a-C-1.0 electrodes at a scan rate of 0.5 mV s^{-1} during the first three cycles.

driven electrolyte degradation.[28] In the second and third discharge, the annealed MoS_2 electrode displays two potential plateaus at about 1.9 and 1.2 V and the potential plateau at about 0.6 V in the first discharge disappears. In the charge (delithiation) process, the annealed MoS_2 electrodes exhibit conspicuous potential plateaus at about 2.2 V because of the high crystallinity of the annealed MoS_2. As shown in Fig. 7(b, c and d), in the first discharge (lithiation) process, the graphene-like MoS_2/a-C electrodes display two inconspicuous potential plateaus at 1.1 and 0.6 V, which is in accordance with those of the annealed MoS_2. The inconspicuous potential plateaus of the discharge of the graphene-like MoS_2/a-C electrodes were caused by low crystallinity, more disorder and dispersion in the amorphous carbon of the graphene-like MoS_2. In addition, the graphene-like MoS_2/a-C electrodes display a potential plateau at about 2.0 V in the first discharge. The potential plateau at about 2.0 V can also be observed in the first discharge curves of amorphous carbon (Fig. 7e). This discharge potential plateau at about 2.0 V should be attributed to the reduction of residual oxygen-containing functional groups of the amorphous carbon. In the first three charge curves, the graphene-like MoS_2/a-C electrodes display an inconspicuous potential plateau at 2.2 V due to the lower crystallinity and more defect sites of the graphene-like MoS_2 in the composites compared to the annealed MoS_2. Cyclic voltammetry (CV) was performed on the graphene-like MoS_2/a-C-1.0 and the first three CV curves are shown in Fig. 7f. During the first cycle, three reduction peaks (~1.2 V, 0.8 V and 0.5 V) and three corresponding oxidation peaks (~1.5 V, ~1.8 V and 2.3 V) can be observed. In the second and third cycle, three pairs of reduction

and oxidation peaks can be observed. There is no significant change in the potentials of the oxidation peaks, but the potentials of the reduction peaks shift from their original positions to ~2.1 V, ~1.2 V and ~0.2 V, which are in accordance with the charge/discharge curves of MoS_2/a-C-1.0. As shown in Fig. 7, in the first cycle, the annealed MoS_2, graphene-like MoS_2/a-C-0.5, MoS_2/a-C-1.0, MoS_2/a-C-2.0 and amorphous carbon electrodes deliver the specific capacity of 653, 748, 926, 559 and 180 mAh g^{-1}, respectively. Among these, MoS_2/a-C-1.0 delivers the highest reversible capacity.

Fig. 8 shows the cycling behaviors of the annealed MoS_2, amorphous carbon and graphene-like MoS_2/a-C composites electrodes. As shown in Fig. 8a, the specific capacity of the annealed MoS_2 electrode reaches the maximum (787 mAh g^{-1}) after 10 cycles, then its capacity obviously decreases with the increasing of cycle numbers, and decreases to 315 mAh g^{-1} after 50 cycles, which is only 40% of the initial capacity. The amorphous carbon electrode exhibits excellent cycle stability, but its capacity is only about 170 mAh g^{-1}. In comparison with the annealed MoS_2 electrode, the graphene-like MoS_2/a-C composite electrodes enhance significantly the cyclic stability. The maximal capacities are up to 776, 961 and 559 mAh g^{-1} for the graphene-like MoS_2/a-C-0.5, MoS_2/a-C-1.0 and MoS_2/a-C-2.0 composites, respectively.

The initial capacity of the graphene-like MoS_2/a-C-0.5 and MoS_2/a-C-2.0 are lower than or approach that of the annealed MoS_2, but is larger than that of the annealed MoS_2 after 40 cycles due to the better cyclic stability of the graphene-like MoS_2/a-C electrodes. Among the samples, the graphene-like MoS_2/a-C-1.0 exhibits the best charge/discharge performances. Its reversible capacity reached its maximum (961 mAh g^{-1}) after several cycles, and a reversible capacity of 912 mAh g^{-1} is still retained after 100 cycles, which corresponds to a capacity retention rate of 95%. According to the weight proportion of MoS_2 in the graphene-like MoS_2/a-C-1.0 (58.35 wt.% MoS_2) and the capacity of the amorphous carbon (180 mAh g^{-1}), it is calculated that the specific capacity of graphene-like MoS_2 in the MoS_2/a-C-1.0 is up to 1518 mAh g^{-1}. It isn't considered that such a high capacity is attributed to only the graphene-like MoS_2 nanosheets. According to the highest specific capacity of the exfoliated MoS_2 (1131 mAh g^{-1}) reported by Lemmon *et al.*,[21] it could be calculated that the capacity of the graphene-like MoS_2/a-C-1.0 composite should be about 735 mAh g^{-1}, which is lower than our measured value of 961 mAh g^{-1}. Therefore, such a high capacity should be attributed to two factors: the MoS_2 graphene-like structure and the synergistic effect between the graphene-like MoS_2 with amorphous carbon. Lemmon *et al.*[21] reported that the exfoliated MoS_2/PEO nanocomposite electrode delivered a very high capacity due to the increased structural disorder and expanded structure of the exfoliated MoS_2 nanosheets. Guo *et al.*[22] also reported that the high capacity of the restacked exfoliated MoS_2 was due to an enlarged *c*-axis parameter. Feng *et al.*[17] suggested that lithium ion could intercalate into the nanoclusters, defect sites, layer sites and hollow core of MoS_2 nanoflakes, which contribute to their high reversible capacity (900~1000 mAh g^{-1}). In this work, XRD and HRTEM demonstrated that the graphene-like MoS_2/a-C composites have larger interlaminar distances between the graphene-like MoS_2 nanosheets. Because the growth of MoS_2 crystals, especially in the (002) plane, was greatly inhibited by the amorphous carbon, the graphene-like MoS_2 nanosheets should have more defect sites. Moreover, more nanoclusters, defect sites and hollow core should exist due to the composite between the graphene-like MoS_2 nanosheets and amorphous carbon. The above factors would greatly enhance the capacity of the graphene-like MoS_2/a-C composites. The composite of graphene-like MoS_2 with amorphous carbon inhibits the restack of the graphene-like MoS_2 nanosheets and stabilizes the electrode structure. Additionally, the amorphous carbon can stabilize the disordered structure of the graphene-like MoS_2 nanosheets throughout the cycling regime to accommodate more Li^+ ions, and also keep the active materials electrically connected. Therefore, graphene-like MoS_2/a-C composites electrodes exhibited a significantly enhanced capacity and excellent cyclic stability. This kind of graphene-like MoS_2/a-C composites with high capacity and excellent stability would find wide applications as a promise anode material for LIB.

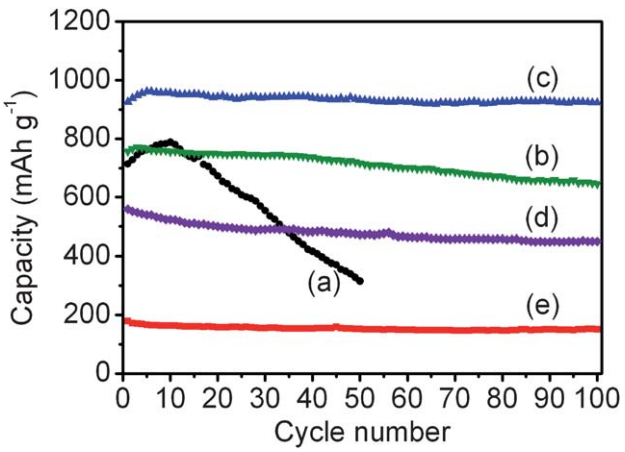

Fig. 8 Cycling behaviour of (a) annealed MoS_2; graphene-like MoS_2/a-C composites with adding (b) 0.5 g, (c) 1.0 g and (d) 2.0 g glucose; (e) amorphous carbon.

Conclusions

This work has developed a facile method to prepare graphene-like MoS_2/a-C composites by a simple hydrothermal method with addition of glucose and then annealing at 800 °C for 2 h under H_2/N_2 atmosphere. The characterization demonstrated that the graphene-like MoS_2 nanosheets dispersed uniformly in amorphous carbon to form graphene-like MoS_2/a-C composites. The mechanism of the formation of the graphene-like MoS_2/a-C includes that the MoS_2 nanowhiskers are highly dispersed in the colloidal carbonaceous produced *in stiu* by the hydrothermal carbonization of glucose, and that after annealing the colloidal carbonaceous is changed to amorphous carbon, which inhibits the crystal growth of MoS_2, especially in the (002) plane. The interlayer distance between adjacent graphene-like MoS_2 nanosheets was about 1.00 nm and the interlayer distance between the MoS_2 layer and the carbon layer was about 0.50 nm. It was demonstrated that the graphene-like MoS_2/a-C composites exhibited high reversible capacity and excellent cyclic stability.

Among the samples, the graphene-like MoS_2/a-C composite delivered the highest reversible capacity (961 mAh g^{-1}), and still retained 912 mAh g^{-1} after 100 cycles. The significant improvements in the electrochemical performances of the composites could be attributed to the unique structure and properties of the graphene-like MoS_2 nanoheets, and the synergistic effect of the graphene-like MoS_2 and the amorphous carbon. The present results suggest that graphene-like MoS_2/a-c composites is a promising material for LIB.

Acknowledgements

This work was supported by the Zhejiang Provincial Natural Science Foundation of China (Y407030, Y4100119), 973 Fundamental Research Program from the Ministry of Science and Technology of China (2010CB635116) and Ph.D Start-up Research Program of Guangdong Natural Science Foundation (10452404801004521).

References

1 J. M. Tarascon and M. Armand, *Nature*, 2001, **414**, 359.
2 J. Breger, Y. S. Meng, Y. Hinuma, S. Kumar, K. Kang, Y. Shao-Horn, G. Geder and C. P. Grey, *Chem. Mater.*, 2006, **18**, 4678.
3 M. Winter and R. J. Brodd, *Chem. Rev.*, 2004, **104**, 4245.
4 J. Chen and F. Cheng, *Acc. Chem. Res.*, 2008, **42**, 713.
5 A. K. Geim and K. S. Novoselov, *Nat. Mater.*, 2007, **6**, 183.
6 E. J. Yoo, J. Kim, E. Hosono, H. S. Zhou, T. Kudo and I. Honma, *Nano Lett.*, 2008, **8**, 2277.
7 G. X. Wang, X. P. Shen, J. Yao and J. Park, *Carbon*, 2009, **47**, 2049.
8 D. H. Wang, R. Kou, D. W. Choi, Z. G. Yang, Z. M. Nie, J. Li, L. V. Saraf, D. H. Hu, J. G. Zhang, G. L. Graff, J. Liu, M. A. Pope and I. A. Aksay, *ACS Nano*, 2010, **4**, 1587.
9 R. Tenne, L. Margulis, M. Genut and G. Hodes, *Nature*, 1992, **360**, 444.
10 Y. F. Li, Z. Zhou, S. B. Zhang and Z. F. Chen, *J. Am. Chem. Soc.*, 2008, **130**, 16739.
11 J. Kibsgaard, J. V. Lauritsen, E. Laegsgaard, B. S. Clausen, H. Topsoe and F. Besenbacher, *J. Am. Chem. Soc.*, 2006, **128**, 13950.
12 Z. Y. Wang, H. Li, Z. Liu, Z. Shi, J. Lu, K. Suenaga, S. K. Joung, T. Okazaki, Z. N. Gu, J. Zhou, Z. X. Gao, G. P. Li, S. Sanvito, E. Wang and S. Lijima, *J. Am. Chem. Soc.*, 2010, **132**, 13840.
13 C. M. Zelenski and P. K. Dorhout, *J. Am. Chem. Soc.*, 1998, **120**, 734.
14 Y. Feldman, E. Wasserman, D. J. Srolovitz and R. Tenne, *Science*, 1995, **267**, 222.
15 P. R. Bonneau, R. F. Jarvis and R. B. Kaner, *Nature*, 1991, **349**, 510.
16 C. Q. Feng, L. F. Huang, Z. P. Guo and H. K. Liu, *Electrochem. Commun.*, 2007, **9**, 119.
17 C. Q. Feng, J. Ma, H. Li, R. Zeng, Z. P. Guo and H. K. Liu, *Mater. Res. Bull.*, 2009, **44**, 1811.
18 H. Li, W. J. Li, L. Ma, W. X. Chen and J. M. Wang, *J. Alloys Compd.*, 2009, **471**, 442.
19 H. S. S. Ramakrishna Matte, A. Gomathi, A. K. Manna, D. J. Late, R. Datta, S. K. Pati and C. N. R. Rao, *Angew. Chem. Int. Ed*, 2010, **49**, 4059.
20 J. W. Seo, Y. W. Jun, S. W. Park, H. Nah, T. Moon, B. Park, J. G. Kim, Y. J. Kim and J. Cheon, *Angew. Chem., Int. Ed.*, 2007, **46**, 8828.
21 J. Xiao, D. W. Choi, L. Cosimbescu, P. Koech, J. Liu and J. P. Lemmon, *Chem. Mater.*, 2010, **22**, 4522.
22 G. Du, Z. P. Guo, S. Wang, R. Zeng, Z. Chen and H. Liu, *Chem. Commun.*, 2010, **46**, 1106.
23 Z. Z. Wu, D. Z. Wang, Y. Wang and A. Sun, *Adv. Eng. Mater.*, 2010, **12**, 534.
24 X. M. Sun and Y. D. Li, *Angew. Chem., Int. Ed.*, 2004, **43**, 3827.
25 K. S. Liang, R. R. Chianelli, F. Z. Chien and S. C. Moss, *J. Non-Cryst. Solids*, 1986, **79**, 251.
26 X. M. Sun and Y. D. Li, *J. Colloid Interface Sci.*, 2005, **291**, 7.
27 R. Dominko, D. Arcon, A. Mrzel, A. Zorko, P. Cevc, P. Venturini, M. Gaberscek, M. Remskar and D. Mihailovic, *Adv. Mater.*, 2002, **14**, 1531.
28 G. X. Wang, S. Bewlay, J. Yao, H. K. Liu and S. K. Dou, *Electrochem. Solid-State Lett.*, 2004, **7**, A321–A323.